

Molecular Dynamics Simulation of a Membrane/Water Interface: The Ordering of Water and Its Relation to the Hydration Force

Siewert-Jan Marrink,[†] Max Berkowitz,^{*,‡} and Herman J. C. Berendsen^{*,†}

BIOSON Research Institute and Laboratory of Biophysical Chemistry, University of Groningen, Nijenborgh 4, 9747 AG Groningen, The Netherlands, and Department of Chemistry, University of North Carolina, Chapel Hill, North Carolina 27599

Received March 16, 1993. In Final Form: June 23, 1993*

In order to obtain a better understanding of the origin of the hydration force, three molecular dynamic simulations of phospholipid/water multilamellar systems were performed. The simulated systems only differed in the amount of interbilayer water, ranging from the minimum to the maximum amount of swelling in the liquid-crystal phase. The analysis of orientational polarization, hydrogen bonding and diffusion rates of the water molecules between the membranes reveals a strong perturbing effect, which decays smoothly and approximately exponentially (with a decay length of about 0.25 nm) toward the middle of the water layer. The electrostatic potential profiles show that the decay of water ordering is directly correlated with the decay of the interfacial dipolar charges. Therefore, the propagation of the ordering of water molecules is not intrinsic to water but is merely determined by the local field from the interfacial charge distribution. The decay of the electrostatic potentials appears to be as a stretched exponential in all simulated systems. This type of decay can be interpreted as normal exponential but with a varying local decay length. We speculate that it is the fractal nature of the membrane surface which results in the stretched exponential behavior. The hydration force, resulting from the ordering of the water molecules between the membranes, will also exhibit this type of decay and is thus dependent on solvent as well as membrane structure.

I. Introduction

The forces acting between membrane surfaces are mainly of four types: van der Waals, electrostatic, undulation, and hydration. The first two are explained by the Derjaguin-Landau-Verwey-Overbeek (DLVO) theory;¹ the third one is explained by a theory proposed by Helfrich.^{2,3} For the fourth one, however, a satisfying theory is still unavailable. This force is called hydration because it is believed to be due to the structure of water between the surfaces.⁴

The van der Waals force is always attractive and displays a power law dependence. The three other forces are repulsive between most membranes. The undulation force also displays a power law dependence, whereas both the electrostatic and hydration force decay exponentially with distance. Electrostatic and undulation forces only describe the interaction between membranes when the separation between surfaces is larger than about 10 molecular solvent diameters. Below this value the hydration force is dominant, for both charged and uncharged membranes.⁴ Maybe the main reason that the hydration force is still not understood lays in the fact that it only acts at short distances. Therefore a continuum description (as can be given for the other forces) breaks down and the molecular details have to be taken into account.

Currently there are some theories being developed which try to incorporate the atomic details of the system.^{5,6} In order to justify the assumptions being made as well as the

predictions that follow from these theories, we performed a series of molecular dynamics (MD) simulations of a lecithin/water multilamellar system in the liquid-crystal phase, including full atomic details. Our work presented here forms an extension of earlier simulations on this system.^{7,8} These simulations were performed in order to develop a realistic model for a biological membrane. The thorough analysis we did convinced us of the reliability of our model. Atom distributions, electron density profile, tail order parameters, area per headgroup, trans/gauche distributions, and more were examined and found to be in good agreement with experimental results. Now we want to use this model to investigate properties and problems which are not well understood. The molecular origin of the hydration force is such a problem where computer simulations can be very helpful. Earlier computer simulations in the field always used simpler models⁹⁻¹³ or were performed in the gel phase.¹⁴

In the next section we will describe the experimental picture of hydration forces and the state of the current theories explaining them. In section III we give a description of the objectives of the computer simulations and the model and methods we used to evaluate them. Section IV shows the results followed by a discussion. Finally we present some conclusions.

II. Hydration Forces

A. Experimental Section. Hydration forces have been measured by using predominantly the surface-force

[†] University of Groningen.

[‡] University of North Carolina.

* Abstract published in *Advance ACS Abstracts*, September 1, 1993.

(1) Verwey, E. J. W.; Overbeek, J. Th. G. *Theory of Stability of Colloids*; Elsevier: Amsterdam, 1984.

(2) Helfrich, W. Z. *Naturforsch.* 1978, 33a, 305.

(3) Helfrich, W.; Servuss, R. M. *Nuovo Cimento* 1984, 3D, 137.

(4) Rand, S. P.; Das, S. P.; Parsegian, V. A. *Chem. Scr.* 1985, 25, 15.

(5) Kornyshev, A. A.; Leikin, S. *Phys. Rev. A* 1989, 40, 6431.

(6) Cevc, G. J. *Chem. Soc., Faraday Trans.* 1991, 87, 2733.

(7) Egberts, E. *Molecular Dynamics Simulation of Multibilayer Membranes Thesis*, University of Groningen, 1988; Chapter IV.

(8) Egberts, E.; Marrink, S. J.; Berendsen, H. J. C. *Eur. Biophys. J.*, in press.

(9) Scott, H. L. *Biochim. Biophys. Acta* 1985, 814, 327.

(10) Kjellander, R.; Marcelja, S. *Chem. Scr.* 1985, 25, 73.

(11) Kjellander, R.; Marcelja, S. *Chem. Phys. Lett.* 1985, 120, 393.

(12) Makovsky, N. N. *Mol. Phys.* 1991, 72, 235.

(13) Granfeldt, M. K.; Miklavic, S. J. *J. Phys. Chem.* 1991, 95, 6351.

(14) Raghavan, K.; Rami Reddy, M.; Berkowitz, M. L. *Langmuir* 1992, 8, 233.

apparatus¹⁵ and by the osmotic stress method^{16,17} with the results displaying good agreement. The general picture that emerges from the experiments is that up to ~ 3 nm lipid bilayers in water repel each other with an (quasi)-exponentially decaying force. The decay constant of the force varies from 0.1 nm to more than 0.3 nm.¹⁸ If the lipids are neutral the repulsion is eventually balanced by the attractive van der Waals forces. If the lipids are charged, the repulsion continues but with a decay constant compatible with the value obtained from the double layer theory. At very small distances, i.e. less than 0.5 nm, steric overlap causes a strong repulsive force which dominates all others.¹⁹

The strength of the hydration force as well as its measured decay lengths strongly depends on the type of lipid and their physical state. For instance, a strong correlation is observed between the total potential difference across the membrane and the swelling limit.²⁰ Furthermore, increase in the area per headgroup (e.g. due to branching, gel-liquid crystal phase transition, or addition of cholesterol) seems to greatly enhance the decay length.¹⁸ The concentration of ions however seems to be less important.²¹ From experiments between smooth (e.g. mica) surfaces²² the molecular nature of the hydration force is reflected in its oscillatory character correlated to the size of the solvent particles. Computer experiments¹⁴ also find these oscillations between lipid bilayers in the gel phase.

The measurements described above have been performed on systems in aqueous solvents, but it is also known that lipid bilayers swell in some other solvents²³ and the results obtained compare quite well with the aqueous case. In addition it is known that hydration forces can be observed to act between other surfaces, e.g. DNA polyelectrolytes²⁴ and polysaccharides.²⁵

All these facts make the interpretation of the hydration force very complicated. Therefore it is no wonder that different approaches to explain the nature of the hydration force exist. These range from "purely solvent"²⁶ to "purely lipid"²⁷ type of models.

As we believe, a combination of these two extremes will be closer to reality. Although no satisfying theory has been published yet, several attempts are currently being made to incorporate both lipid and solvent details into one model.^{5,6} We will discuss them below and give our interpretation of them.

B. Theory. Purely Solvent Model. Nearly immediately after the publication of the first data on the hydration force,¹⁶ Marcelja and Radic (MR)²⁶ proposed a theory in order to explain the nature of the observed strong force. According to MR theory the force is due to the modification of water structure at the membrane/water interface. Near the interface the water molecules are different from the

water molecules in the bulk; they are more "ordered". To describe this "order" one can introduce an order parameter $\eta(z)$ and perform a Landau-type expansion of the free energy density $g(z)$, i.e. write that

$$g(z) = g_0 + a\eta(z)^2 + c(\partial\eta(z)/\partial z)^2 + \dots \quad (1)$$

where g_0 is the free energy density in bulk water and a and c are constants. The behavior of the order parameter follows from minimization of the free energy density and leads to the following expression of the repulsive pressure p between two interfaces at a distance h

$$p = 4p_0 \exp(-h/\lambda) \quad (2)$$

where $\lambda = (c/a)^{1/2}$ and $p_0 = a\eta^0^2$. The value of p_0 (the pressure when the surfaces are at close contact) is determined by the extent to which the surface orders the water and, therefore, depends on the properties of the surface. The decay parameter λ is determined by the extent to which the ordering is propagated through water and therefore, according to the MR theory, is a property of water only.

Since the Landau type expansion has an empirical character, it is important to justify it on molecular grounds. Gruen and Marcelja,^{28,29} as well as Kornyshev,³⁰ made an attempt to do this and discovered that they had to assume that the polarization of water is nonlocal. From the minimization of the free energy density the following form for the dielectric function $\epsilon(k)$ can be obtained

$$\epsilon(k) = \epsilon_\infty + \frac{\epsilon_0 - \epsilon_\infty}{1 + \lambda^2 k^2 \epsilon_0 / \epsilon_\infty} \quad (3)$$

where k is the wavelength, ϵ_0 and ϵ_∞ are the static and high-frequency dielectric constants, respectively, and λ is a decay length the value of which is fixed to secure agreement with the measured forces. The theoretical background for this needs to be questioned, however. Attard *et al.*³¹ showed that the assumption of a nonlocal dielectric function is incorrect. Recently, Kornyshev *et al.*³² have shown that Attard's criticism is not necessarily correct; hence the dielectric function given by eq 3 may well be a good first approximation for the description of hydration phenomena. The above described free energy approach however remains mainly phenomenological and its physical interpretation unclear.

Surface Correlations. Although elegant and simple, the largest flaw of the free energy approach is that the decay constant is independent of the nature of the surface. The experimental data show that this is not the case. Recently, Kornyshev and Leikin (KL)⁵ extended the MR theory and demonstrated how this dependence can be explained. They replaced the homogeneous boundary conditions used in the MR theory by inhomogeneous ones. These boundary conditions were set up such as to mimic the lateral correlations between the (dipolar) charges at the surfaces. Showing that only correlations between charges at the same surface contribute to the repulsion force, they finally derived an expression for the repulsive pressure similar to eq 2, the main result of MR theory

$$p = p_0 / \sinh^2[\lambda_{\text{eff}} h / 2] \quad (4)$$

Here the decay length λ_{eff} is an effective one, depending

(15) Marra, J.; Israelachvili, J. N. *Biochemistry* 1985, 24, 4608.

(16) LeNeveu, D. M.; Rand, R. P.; Parsegian, V. A. *Nature* 1976, 259, 601.

(17) McIntosh, T. J.; Simon, S. A. *Biochemistry* 1986, 25, 4058.

(18) Rand, R. P.; Parsegian, V. A. *Biochim. Biophys. Acta* 1989, 988, 351.

(19) McIntosh, T. J.; Magid, A. D.; Simon, S. A. *Biochemistry* 1987, 26, 7325.

(20) Simon, S. A.; McIntosh, T. J. *Proc. Natl. Acad. Sci. U.S.A.* 1989, 86, 9263.

(21) Lys, L. J.; Lys, W. T.; Parsegian, V. A.; Rand, R. P. *Biochemistry* 1981, 20, 1771.

(22) Christenson, H. K.; Horn, R. G.; Israelachvili, J. N. *J. Colloid Interface Sci.* 1982, 88, 79.

(23) McIntosh, T. J.; Magid, A. D.; Simon, S. A. *Biochemistry* 1989, 28, 7904.

(24) Rau, D. C.; Lee, B.; Parsegian, V. A. *Proc. Natl. Acad. Sci. U.S.A.* 1984, 81, 2621.

(25) Rau, D. C.; Parsegian, V. A. *Science* 1990, 249, 1278.

(26) Marcelja, S.; Radic, N. *Chem. Phys. Lett.* 1976, 42, 129.

(27) Israelachvili, J. W.; Wennerström, H. *Langmuir* 1990, 6, 873.

(28) Gruen, D. W. R.; Marcelja, S. *J. Chem. Soc., Faraday Trans. 2* 1983, 79, 211.

(29) Gruen, D. W. R.; Marcelja, S. *J. Chem. Soc., Faraday Trans. 2* 1983, 79, 225.

(30) Kornyshev, A. A. *J. Chem. Soc., Faraday Trans. 2* 1983, 79, 651.

(31) Attard, P.; Wei, D.; Patey, G. N. *Chem. Phys. Lett.* 1990, 172, 69.

(32) Kornyshev, A. A.; Kossakowski, D. A.; Vorotyntsev, M. A. *Condensed Matter Physics Aspects of Electrochemistry*; Tosi, M. P., Kornyshev, A. A., Eds.; World Scientific: Singapore, 1991; p 92.

on the mutual proportions of the "intrinsic" water decay length and the characteristic length and width of the surface correlations. Therefore, according to KL theory, the decay length of the hydration force does depend on the nature of the interface. As Kornyshev and Leikin show the assumptions they made are able to explain at least some of the experimental data.

Surface Width. Both MR and KL models however consider the membrane/water interface to be infinitely small. No smearing out of charges in the direction perpendicular to the surface is allowed. Various experiments clearly indicate the existence of a broad interface.³³⁻³⁵ A flat interface is definitely an oversimplification, but the question is how much it will influence the hydration pressure. The most radical point of view was taken by Israelachvili and Wennerström (IW)²⁷ who assumed that the hydration force has nothing to do with water but is a result of the smearing out of the interface only. Based on a very simple model of protruding lipids, they showed that an exponentially decaying repulsive force could result just from the entropic confinement of lipids at opposing membranes. By use of this model, some of the experimental data which could not be explained by MR theory could now be clearly understood.²⁷ Others, however, became suddenly less obvious.³⁶

In our point of view therefore, the interfacial width has definitely to be taken into account, but without abandoning the role of the solvent. An attempt in this direction is currently being made by Cevc.⁶ In his work he tries to treat the screening of surface charge distribution by water molecules analogous to the screening of a charged surface by ions in the well-known electrostatic double layer theory of Gouy and Chapman.^{37,38} Instead of real charges on the surface and ions in solution, he assumes "surface-associated local-excess charges" $\rho_p(z)$ being compensated by "solvent-associated local excess charges" $\rho_h(z)$. The surface charges are not fixed in a plane but smeared out in the direction perpendicular to the surface. Analogous to the Gouy-Chapman theory he then derives the following expression for the total potential near a polar surface

$$\psi(z) = \frac{\lambda}{\epsilon_\infty \epsilon_0} (-0.5 \int_0^\infty \rho_p(z') \exp[(z-z')/\lambda] dz' + \int_0^z \rho_p(z') \sinh[(z-z')/\lambda] dz') \quad (5)$$

The potential depends both on the solvent structure (again by means of some "intrinsic" decay length λ) and on the interfacial structure (by means of $\rho_p(z)$). The same will hold also for the other hydration-dependent thermodynamic quantities, like the hydration pressure, which analogous to Gouy-Chapman theory can be obtained from eq 5 by integration. To solve eq 5, one needs to know how the surface-associated local-excess charges are distributed. The simplest case is assuming an exponentially decaying interface, which will result in an exponential decay of the hydration force with two decay lengths, one due to water and the other directly reflecting the decay of the interface itself. Other, more realistic, surface charge distributions result in more complicated expressions.

C. Qualitative Model. Based on the theories and experimental data as described above, the qualitative picture we have in mind is the following: the hydration

force is a result of the ordering of solvent molecules due to the presence of two interfaces. It is therefore in the first place an entropic repulsion, as in the case of the overlap between two electrical double layers. Direct electrostatic interactions can even be attractive in the case of favorable charge correlations.³⁹ The total hydration free energy (and therefore the resulting hydration force) will depend on an interplay between (at least) three basically different types of mechanisms: one describing the nature of the solvent, another describing the lateral surface-charge correlations, and a third for the perpendicular surface-charge distribution. It is not surprising that the exact expression will be rather complicated, involving all types of cross correlations. Almost certainly, these will give rise to a more complicated decay than a simple exponential. Of course, for systems where one contribution dominates the others, a large simplification can be made. But still a simple exponential decay would be fortuitous instead of naturally occurring. For instance, the most natural assumption to be made for an interface is that it has a Gaussian decay instead of an exponential one, and therefore (see Cevc's theory⁶) this will be reflected in the hydration force also. The same holds for the contribution of the surface correlations, which already in the simple KL model show combined exponential behavior. The form of an "intrinsic" water decay remains unclear, and so does its value. This is reflected in the large spread of experimentally observed "intrinsic" decay lengths, which can be as small as 0.075 nm,⁶ or may have the value of ~ 0.2 nm related to the molecular size of water^{18,26} and even become larger than 0.4 nm!¹⁵ Considering the complications, any quantitative estimate of hydration forces based on current theories remains highly questionable. The simple single exponential decay as observed experimentally might as well be only a first-order approximation. The apparent decay length then has to be interpreted as an effective one. The noise in the experimental data prohibits a more detailed analysis, however.

III. Computer Simulations

A. Objectives. It seems that the aid of computer simulations can be very fruitful in elucidating what is happening at the water/membrane interface on the molecular level. Questions we would like to address in our simulations are as follows: (1) How much do lipids protrude? (2) How does the interface decay? (3) How much is the water being ordered? (4) Does the water exhibit any intrinsic decay? (5) Do we observe an oscillatory or smooth structure of water? (6) What do the electrostatic potentials look like? (7) What determines the decay of the hydration force? Of course, the results of our simulations only directly apply to a bilayer of lecithins in the liquid-crystalline phase, but from this and from comparison to other simulations we can get also some more general ideas about the nature of the hydration force.

Originally we had the idea of computing the chemical potential of the interbilayer water molecules. This should be a direct measure of the hydration force, which is the derivative of this chemical potential. Unfortunately, current free energy methods are only accurate to about 0.5 kJ/mol. This is approximately equal to the total free energy difference to be expected going from an almost dry to a fully swelled bilayer.¹⁸ Therefore such a very time-consuming calculation would not have been meaningful at all.

B. Method and Model. As mentioned in the introduction, the work we present here is based on the earlier simulations of a lipid membrane.^{7,8} The model membrane

(33) Büldt, G.; Gally, H. U.; Seelig, J. *J. Mol. Biol.* 1979, 134, 673.

(34) Zaccai, G.; Blasie, J. K.; Schoenborn, B. P. *Proc. Natl. Acad. Sci. U.S.A.* 1980, 72, 376.

(35) Pfeiffer, W.; Henkel, Th.; Sackmann, E.; Knoll, W.; Richter, D. *Europhys. Lett.* 1989, 8, 201.

(36) Parsegian, V. A.; Rand, R. P. *Langmuir* 1991, 7, 1299.

(37) Gouy, G. *J. Phys. (Paris)* 1910, 9, 457.

(38) Chapman, D. L. *Philos. Mag.* 1913, 25, 475.

(39) Attard, P.; Mitchell, D. J. *J. Chem. Phys.* 1988, 88, 4391.

system we use consists of 64 dipalmitoylphosphatidylcholine (DPPC) lipid molecules arranged in a bilayer, separated by 736 water molecules (11.5 per lipid, water weight fraction $c = 0.22$). Periodic boundary conditions are applied in all three dimensions, so actually a multilamellar system is represented. Both constant temperature and constant pressure are maintained by coupling to a temperature bath of $T = 350$ K and by anisotropic coupling to a reference pressure of $P = 1$ atm.⁴⁰ The timestep of integration was set to 2 fs. Bond lengths were constrained by the SHAKE method.^{41,42} We used the GROMOS⁴³ simulation package and force field which is all-atom except for methyl groups which are treated as united atoms. The water is modeled as SPC.⁴⁴ Some modifications to the standard force field had to be made to ensure the system to be in the liquid-crystalline phase. The cutoff for Lennard-Jones interactions was 0.85 nm. Electrostatic interactions were updated every 10th timestep using a cylindrical cut-off with radius 1.7 nm in the plane parallel to the membrane surface. In the perpendicular direction all interactions were taken into account. A more elaborate description of all parameters (including the complete force field) is given elsewhere.^{7,8}

We also set up two new systems which differ from the original one only in the amount of interbilayer water. They were generated by inserting a slab of equilibrated SPC water into the equilibrated old system. After energy minimization, an 80-ps run was performed to let the system adopt to its new equilibrium values. The reaching of equilibrium was deduced from the stabilization of cell parameters and energies and was furthermore checked by analyzing various properties over different time frames during the subsequent 80-ps production runs. For the simulation with the largest amount of water, we increased the electrostatic cylindrical cutoff radius parallel to the membrane surface to 2.0 nm. This had a small effect on the ordering of water molecules in the center of the water layer. Some test runs on the other systems (those with fewer waters) showed no noticeable effects upon enlargement of the cutoff radius. We thus finally analyzed 80-ps trajectories of three systems at different water weight fractions, c : (1) small water layer, labeled "S", old system, $c = 0.22$ (11.5 waters/lipid); (2) medium water layer, labeled "M": new system, $c = 0.39$ (20.5 waters/lipid); (3) large water layer, labeled "L": new system, $c = 0.56$ (29.1 waters/lipid). The amount of water in the S simulation is about the minimum to keep a stable liquid-crystalline phase, and the L simulation is just above the swelling limit.

The analysis we performed on these three systems includes the computation of atom distributions, hydrogen bonding, orientational polarization, electrostatic potential, and diffusion rates. Since these properties had to be calculated as a function of position along the membrane normal, we divided our system up into slices. Per slice the averaging was done separately, thus creating histograms. The width of the slices was chosen such as to minimize the noise, but without losing details. Considering the symmetry of the system with respect to the middle of the water layer, all data were averaged over the two interfaces in order to improve the statistics.

IV. Results

In this section we present the results of our simulations which we think will contribute to the understanding of the hydration force. First, in subsection A, we describe some properties of the lipid membrane itself. These comprise the bilayer parameters (e.g. area/headgroup, bilayer repeat distance), the interfacial structure (atom distributions), and interfacial mobility. In subsection B, the ordering of the water molecules between the bilayers is analyzed. This is done through the evaluation of hydrogen bonding patterns, diffusion rates, and polarization. Finally, in subsection C, the electrostatic potential across the membrane interfaces is presented.

A. Membrane Properties. Bilayer Parameters. The original system (simulation S, with small water layer) has an equilibrium area per headgroup of 0.575 nm^2 , which is very close to reported ones (around 0.59 nm^2) for DPPC under similar conditions.^{45,46} The bilayer repeat distance of 5.6 nm is at the higher end of the experimental data,^{33,47-49} ranging from 5.25 to 5.6 nm. Both larger systems experienced swelling in the lateral direction, resulting in a larger area per headgroup of 0.64 nm^2 . This swelling is also observed experimentally,^{18,50,51} values ranging from 0.64 to 0.68 nm^2 . The bilayer repeat distances have increased to 6.2 and 7.1 nm for the M and L simulations, respectively. Experimental measurements give 6.0 nm at $c = 0.43$ ⁵⁰ and 6.7 nm at $c = 0.54$.¹⁸ Converted to our water weight fraction (assuming a bulk value for the water density), one would expect bilayer repeat distances close to our values.

Interfacial Structure. The most obvious thing to look at, and easily obtained from computer simulations, is the average distribution of atoms across the system. The interfacial distribution of nitrogen, phosphorus, and carbonyl groups together with water is plotted in Figure 1, for S, M, and L simulations separately. In all three simulations we observe a broad interface. Defining an interfacial width as the distance over which the water density drops from 90% to 10%, we find it to be close to 1.0 nm in all simulations. Water penetrates up to the carbonyl groups and there is still noticeable headgroup density in the water layer. Only the L simulation has a small slice of pure water, with a density equal to the density of bulk SPC water.⁵² The relative penetration of headgroups into water is largest in the S simulation, which causes a somewhat larger bilayer thickness. The scatter in computed bilayer thickness from experimental measurements^{18,53} makes it unclear whether this is a real feature at low water weight fraction or that it is an artifact of our simulations.

The mutual distribution of the phosphorus and nitrogen atoms does not vary significantly in our simulations, nor does the width of their distributions. The dipole vector connecting the phosphorus and nitrogen atoms has an average orientation of 20° with respect to the bilayer surface, independent on thickness of the water layer. The

(40) Berendsen, H. J. C.; Postma, J. P. M.; van Gunsteren, W. F.; Dinola, A.; Haak, J. R. *J. Chem. Phys.* 1984, 81, 3684.

(41) van Gunsteren, W. F.; Berendsen, H. J. C. *Mol. Phys.* 1977, 34, 1311.

(42) Ryckaert, J. P.; Ciccoliti, G.; Berendsen, H. J. C. *J. Comp. Phys.* 1977, 25, 237.

(43) van Gunsteren, W. F.; Berendsen, H. J. C. *GROningen MOlecular Simulation*, software package, University of Groningen, 1987.

(44) Berendsen, H. J. C.; Postma, J. P. M.; van Gunsteren, W. F.; Hermans, J. *Intermolecular Forces*; Pullman, B., Ed.; Reidel: Dordrecht, 1981; p 331.

(45) Phillips, M. C.; Williams, R. M.; Chapman, D. *Chem. Phys. Lipids* 1974, 3, 234.

(46) Träuble, H.; Haynes, D. H. *Chem. Phys. Lipids* 1974, 7, 324.

(47) Levine, Y. K.; Wilkins, M. H. F. *Nature, New Biol.* 1971, 230, 89.

(48) Chapman, D.; Williams, R. M.; Ladbroke, B. D. *Chem. Phys. Lipids* 1967, 1, 445.

(49) Janiak, M. J.; Small, D. M.; Shipley, G. G. *Biochemistry* 1976, 15, 4575.

(50) Ruocco, M. J.; Shipley, G. G. *Biochim. Biophys. Acta* 1982, 691, 309.

(51) Lewis, B. A.; Engelman, D. M. *J. Mol. Biol.* 1983, 166, 211.

(52) Postma, J. P. M. *A Molecular Dynamics Study of Water*, Thesis, University of Groningen, 1985.

(53) Nagle, J. F.; Wiener, M. C. *Biochim. Biophys. Acta* 1988, 942, 1.

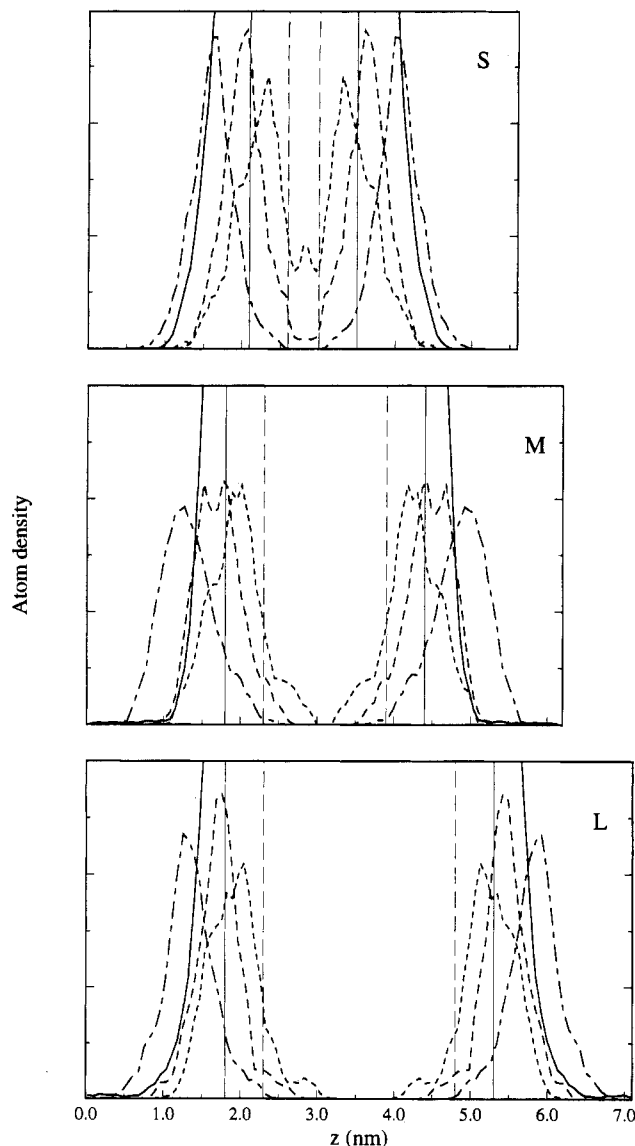


Figure 1. Distribution of interfacial atom types: water (solid), nitrogen (dashed), phosphorus (long dashed), and carbonyl (dot dashed). Interfacial planes (solid) and border planes (dashed) are indicated.

dipole lying close to the surface (instead of pointing outward) agrees with the experimental picture.⁵⁴

In the remaining part of the paper we will relate the properties of the system with respect to a hypothetical interfacial plane, being in some sense the "mid" of the interface. For this we chose the plane going through the center of the average P and N distributions. This also coincides with the peak in the computed electron density profiles (not shown). The location of the "border" plane of the membrane, as used in experimental studies,¹⁷ is defined as a shift of 0.5 nm away from the interfacial plane toward the water layer. The width of the water layer (or distance between the membranes) is taken as the distance between the two "border" planes. Applying this to our systems, we find distances between the "border" planes to be 0.4, 1.6, and 2.5 nm for the S, M, and L simulation, respectively. The position of both the "interfacial" and "border" planes is also indicated in Figure 1. The position of the planes is further illustrated by a graphical picture (Figure 2) of one of the systems (M). Figure 2 also shows clearly the roughness of the membrane/water interface.

To measure the decay of the interface, we considered

the distribution of the choline groups, which protrude furthest into the solvent. Their distributions with respect to the interfacial plane are shown in Figure 3. The curves are very similar in all three different simulations. Due to overlap with the opposing interface, the nitrogen density does not decay to zero in the S simulation. The interfaces in the M simulation are "touching", not overlapping. The decay lengths of the nitrogen distributions were calculated for the M and L simulations, starting from the "border" plane. Although statistical accuracy in this region is not very high, we still can get a rough estimate of the decay lengths. Fitting to a single exponential resulted in decay lengths of 0.24 ± 0.04 nm and of 0.22 ± 0.04 nm in the M and L simulations, respectively. The curves could also be fit to a Gaussian with about the same accuracy, however.

Interfacial Mobility. In order to get some insight about the mobility of the interface and its dependence on the width of the water layer, we looked at the diffusion rates of lipid molecules as well as lipid headgroups in all three simulations. The diffusion rate D of particles can be easily obtained in MD simulations from the slope of the mean square displacement (MSD) curve

$$D = \lim_{t \rightarrow \infty} \frac{\langle [r(t) - r(0)]^2 \rangle}{2dt} \quad (6)$$

Here $r(t)$ stands for the position vector of a particle at a certain time. The brackets denote an ensemble average. The factor d is equal to the number of dimensions which are considered ($d = 1$ for linear, $d = 2$ for lateral, and $d = 3$ for bulk diffusion). Since the diffusion of lipids is a slow process (in the order of 10^{-7} – 10^{-8} cm^2/s ^{55–57}), our simulation time is not sufficient to obtain accurate values for the long time diffusion rates. However, short time diffusion rates (within ± 10 ps), characterizing the motion of lipids within their local potential wells, can be used as a measure for the mobility of the interface. The MSD curves of the lipids as a whole (in z -direction only) and of the headgroups (averaged over all directions) are shown in Figure 4. We see that the interfacial mobility does not depend significantly on the amount of interbilayer water. For the lipids, we calculated short time diffusion rates perpendicular to the membrane surface of $6(\pm 1) \times 10^{-6}$ cm^2/s . Neutron diffraction data on DPPC under conditions close to our S simulation give exactly the same value.⁵⁸ Headgroups, having more freedom, are more mobile. Their (constrained) short time diffusion rate with respect to the center of mass of the lipid is $10(\pm 1) \times 10^{-6}$ cm^2/s (lateral as well as perpendicular).

B. Ordering of Water. To characterize the ordering of water (or the way in which it differs from the bulk), we calculated the following properties: hydrogen bonding, mobility, and polarization. Together these properties will give some description of the otherwise ill-defined "order" property.

Hydrogen Bonding. The number of hydrogen bonds between a water molecule and its neighboring water molecules were calculated using a cutoff criterium of 10 kJ/mole for the pair energy, in order to compare to values obtained from bulk SPC simulations.⁵² Since headgroup density is nonzero almost across the entire water layer, the number of hydrogen bonds in first instance just reflects the water density profile. Therefore we divided the number of hydrogen bonds per water molecule in the slice

(55) Smith, B. A.; McConnell, H. M. *Proc. Natl. Acad. Sci. U.S.A.* 1978, 15, 2759.

(56) Vaz, W. L. C.; Stümpel, J.; Hallmann, D.; Gambacorta, A.; De Rosa, M. *Eur. Biophys. J.* 1987, 15, 111.

(57) Lindblom, G.; Wennerström, H. *Q. Rev. Biophys.* 1977, 10, 67.

(58) König, S.; Pfeiffer, W.; Bayerl, T.; Richter, D.; Sackmann, E. *J. Phys. II* 1992, 2, 1589.

(54) Seelig, J. *Biochim. Biophys. Acta* 1978, 515, 105.

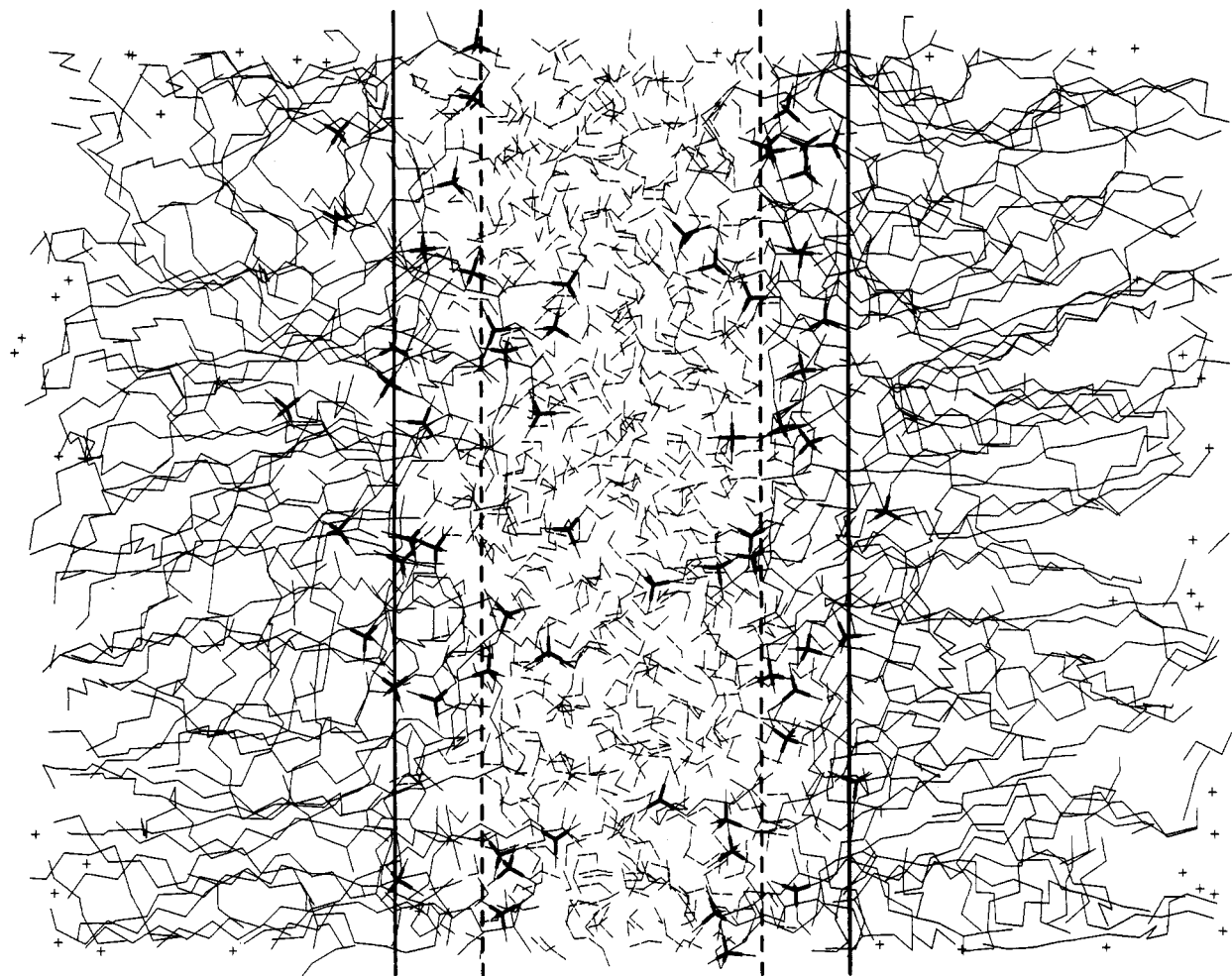


Figure 2. Snapshot of M simulation with indication of "interfacial" planes (solid) and "border" planes (dashed). Thick lines are used for choline groups.

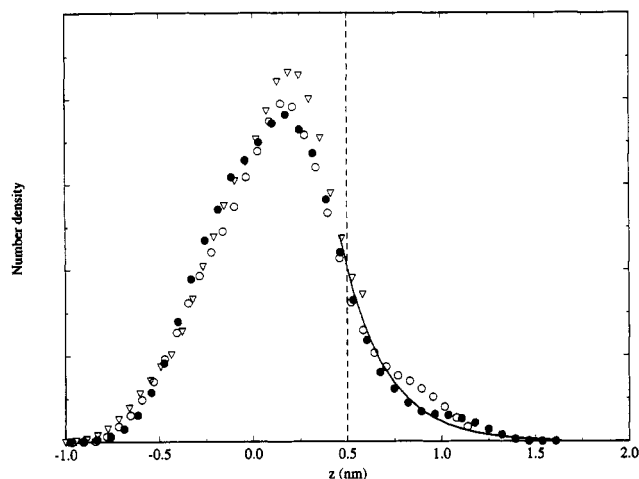


Figure 3. Distribution of nitrogen atoms with respect to the interfacial plane, in different systems: S (triangles), M (open circles), L (solid circles). Border plane (dashed) and the exponential fit (solid) from this plane are also shown.

by the number of neighbors per water molecule in the same slice. The number of nearest neighbors for a specific water molecule is found by counting the number of water molecules within a sphere of radius 0.36 nm (corresponding to the first minimum of the radial distribution function). The described ratio will be a true reflection of the water-water hydrogen bonding structure. It is shown in Figure 5a for all three simulations. The differences among the three systems is negligible. It is clear that the ability of making hydrogen bonds with other water molecules

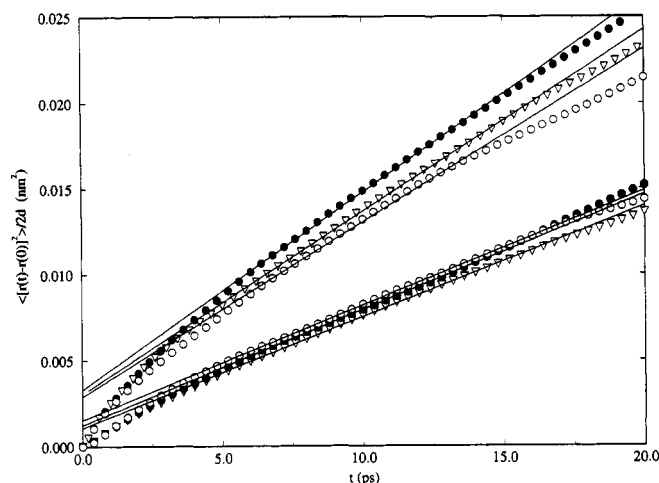


Figure 4. Mean square displacement curves for lipids (lower set) and headgroups (upper set) in different simulations: S (triangles), M (open circles), L (solid circles). The solid lines indicate linear fits over the range $t = 5-15$ ps.

increases toward the membrane. Especially within the interface, water molecules have an enhanced ability to bind to each other. Away from the interface, the effect disappears rapidly, reaching a value close to bulk SPC (0.56).⁵² Fitting the curves from the border plane to an exponential yields a decay length of 0.27 ± 0.03 nm. In order to see whether there is a noticeable structural difference between bulk SPC water and the interstitial SPC water, we examined the hydrogen bonding network. To do this we computed the distributions of the water

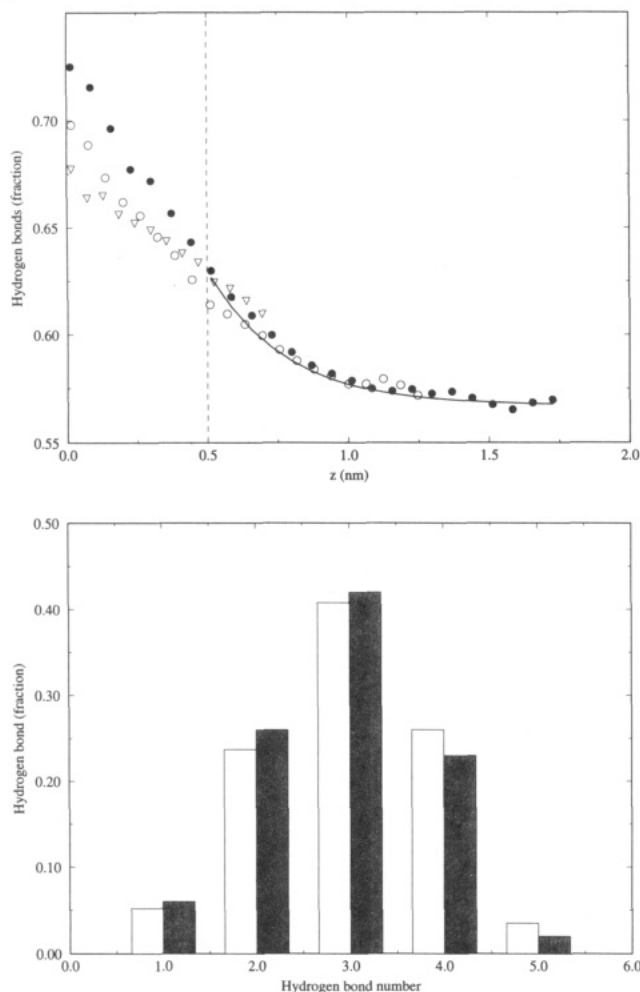


Figure 5. (a, top) Distribution of the average fraction of hydrogen bonds for water molecules with respect to the interfacial plane, in different systems: S (triangles), M (open circles), L (solid circles). Border plane (dashed) and the exponential fit (solid) from this plane are also shown. (b, bottom) Hydrogen bond distribution in middle of water layer of system L (light) and of bulk SPC (dark).

molecules having n hydrogen bonds, with n ranging from 0 to 5. From these we can say that there is a small difference between bulk SPC and "bulk" water in the middle of the water layer in the L simulation (Figure 5b). In the L simulation, the chance of finding 4- and 5-hydrogen bonded water molecules is enhanced, at the cost of 3- and 2-hydrogen bonded ones. The difference is statistically significant. The same trend is seen in the other simulations as well. The large decrease in hydrogen bonding next to gel phase lipids, as observed by MD simulations,¹¹ is contrary to what we see in our simulations. The reason for this we attribute to the broadness of our interface.

Mobility. The diffusion rates of water molecules can in principle be calculated from the slope of the MSD curve (eq 10). Division of the system into slices poses a problem, however, since moving particles do not tend to stay in a particular slice. In order to restrict the crossing of slice boundaries in an unbiased way, we took into account only diffusion within short time intervals (3 ps), neglecting the initial non-Brownian motion.

The dependence of the diffusion coefficient on position in the water layer is plotted in Figure 6, for all three simulations. Since the diffusion rates in lateral and perpendicular direction did not differ significantly, only the total rate is shown. The difference among the simulations remains within the noise. It is clear that the

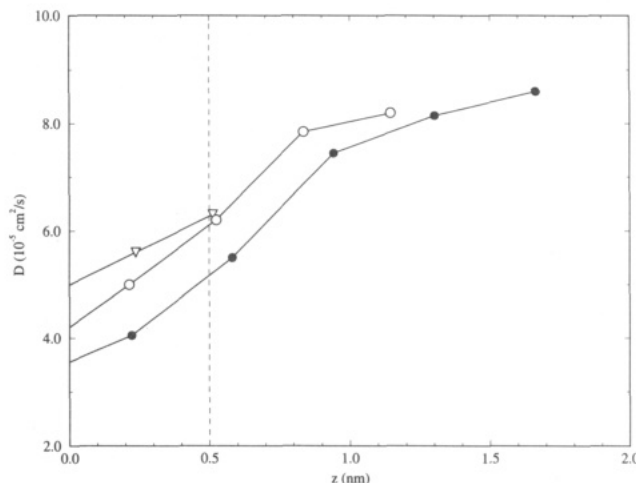


Figure 6. Diffusion rates of water molecules at positions relative to the interfacial plane, in different systems: S (triangles), M (open circles), L (solid circles). Border plane (dashed) is also shown.

mobility of the water molecules increases away from the interface, reaching the diffusion rate of bulk SPC water ($7.5 \times 10^{-5} \text{ cm}^2/\text{s}$ at 349 K).⁵² One should realize that the calculation of a diffusion coefficient in a slice is not very accurate. Therefore the apparent overshoot of the value of the diffusion in the middle of the water layer in M and L simulations may be due to the noise in the calculation.

A separate study on the permeation of water through the membrane⁵⁹ already showed that the slowing down of the water molecules near the interface is caused by the presence of headgroup atoms. Their partial charges invoke large hydration shells, thereby immobilizing the hydrated water molecules.

Polarization. The orientational polarization of water was originally identified^{28,29} as the "order" parameter in the Landau-type expansion of the free energy density (eq 1). Although this phenomenological approach is definitely an oversimplification, the orientational polarization remains the most direct way to characterize the order.

The orientational polarization was calculated by taking the cosine of the angle between the water dipole vector and the membrane normal, i.e. the projection of a unit vector in the dipole direction onto the membrane normal. A positive value indicates an orientation with the dipole pointing toward the membrane. The results are plotted in Figure 7. The polarization profiles exhibit an exponential decay from the surface that is similar in all three simulations. The water orientation becomes random in the middle of the water layer (or at least too small to be separated from the noise) in both M and L simulations. As is to be expected, the polarization is largest in the interfacial region where the charge density is largest. The orientation of water is such as to compensate for the P-N dipole of the headgroup, thus with hydrogen atoms pointing toward the membrane. Although the curves have a considerable noise, we do not see any obvious oscillations as have been observed in previous simulations of gel phase membranes.^{10,11,14} Likely a combination of larger protrusions, higher mobility, and higher temperature result in an averaging out of the solvent details in the liquid-crystalline phase. The polarization profiles can all be fit fairly well by an exponential (starting at the "border" plane) with a decay length of 0.22 ± 0.03 nm.

For comparison, we also included the polarization decay of water between glycolipid membranes (the details of

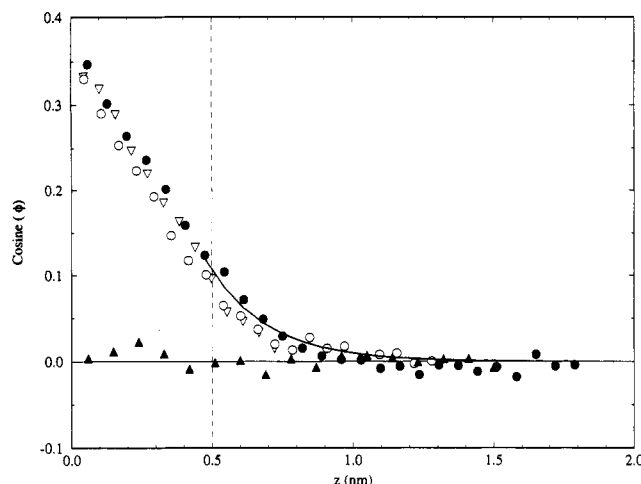


Figure 7. Orientational polarization profile of water molecules at positions relative to the interfacial plane, in different systems: S (open triangles), M (open circles), L (solid circles), and glycolipids (solid triangles). Border plane (dashed) and the exponential fit (solid) from this plane are also shown.

these simulations will be reported elsewhere⁶⁰. The main difference between the glycolipid system and the phospholipid ones is that the former one possesses smaller surface dipoles and an interface which is not as broad. The effect of these differences on the polarization profile is clear. The absence of polarization of the water molecules however does not automatically mean that the glycolipids are not hydrated. On the contrary, clear first and second hydration shells are observed for the glycolipid headgroup atoms.⁶⁰ The polarization of water next to a rather smooth decane layer⁶¹ is also much smaller compared to the polarization we observe next to our membrane. In absence of any charges, only geometrical constraints will play a role which seem to be much weaker than the electrostatic constraints.

C. Electrostatic Potential. The ordering of water molecules as described in the previous section is of course being caused by the disturbing presence of (two) membrane surfaces. As we already observed for the orientational polarization of the water molecules, the presence of a (partial) charge density must influence this ordering significantly. In order to investigate the role of charges, we calculated the electrostatic potential across the interface and water layer. It can be obtained easily from the simulations through the numerical evaluation of the double integral of the charge density

$$\psi(z) - \psi(0) = \int_0^z dz' \int_0^{z'} \rho(z'') dz'' \quad (7)$$

MD computer simulations allow for the "unphysical" splitting of this potential into its constituent parts, the lipid and water molecules separately. The results (lipid, water, and total electrostatic potential) are shown in Figure 8. We note that this potential is the electrostatic potential consistent with the computed charge density using Poisson's equation, without using a cutoff radius as in the simulations.

The lipid potential is built up across the interface and has a positive sign in the water layer compared to inside the membrane. This must be so since the P-N dipole vector is pointing toward the water layer. The contribution to the lipid potential of other charges in the lipid (such as carbonyl dipole) appeared to be very small. The

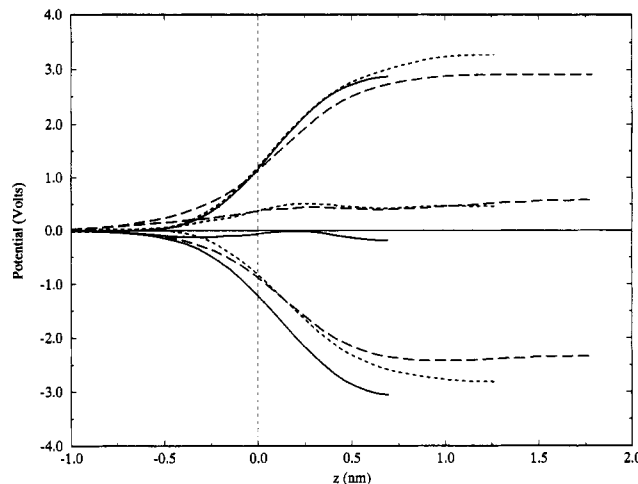


Figure 8. Electrostatic potentials across the interface for headgroups (upper set), water (lower set), and total membrane (middle set), in different systems: S (solid), M (dashed), L (long dashed). Position is relative to the interfacial plane (dashed).

potential levels off toward the bulk, analogous to the nitrogen distribution (compare Figure 3).

The potential of water is almost an exact mirror image of the lipid potential, which means that the lipid charge density is almost completely compensated by the opposed net charge density due to the orientation of the water dipoles, as is to be expected from a high dielectric medium. More interesting, however, is that almost complete compensation occurs everywhere in the interface. The same effect was observed in a simulation of sodium decanoate/decanol/water.⁶²

Therefore, the total potential arising from both lipid and water charges remains rather small. Interesting is the difference between the S simulation, on one hand, and the M and L simulations, on the other. Whereas in the S simulation the total potential is negative, which means that the water molecules actually overcompensate for the lipid dipolar charges, in the other two simulations the lipid potential wins. This effect can be understood from our simulations by looking at the relative penetration depth of water with respect to the headgroups (see Figure 1). The penetration is larger in the S simulation, which means that more water molecules can compensate for charges that are buried deeper in the membrane.

Experimental measurements on lecithin monolayers⁶³ as well as bilayers^{19,64,65} show that the total potential across the interface is negative, its value being between 200 and 500 mV depending on the type of the measurement. This matches our result for the S simulation quite nicely. It also shows that water overcompensation, instead of the carbonyl dipole as is also assumed,^{66,67} can indeed be the cause of the negative total potential. This cannot be derived directly from experiments. The positive total potential observed in the other simulations may well be due to the fact that the small total potential results from the near-compensation of two large potentials and will be sensitive to details of the simulation parameters such as the cutoff method used. Actually, the same feature was

(62) Egberts, E.; Berendsen, H. J. C. *J. Chem. Phys.* 1988, 89, 3718.

(63) Knobler, C. M. *Adv. Chem. Phys.* 1990, 77, 397.

(64) Flewelling, R. F.; Hubbell, W. L. *Biophys. J.* 1986, 49, 541.

(65) Gawrisch, K.; Ruston, D.; Zimmerberg, J.; Parsegian, V. A.; Rand, R. P.; Fuller, N. *Biophys. J.* 1992, 61, 1213.

(66) McLaughlin, S. *Current Topics in Membranes and Transport*; Bronner, F., Kleinzeller, A., Eds.; Academic Press: New York, 1977; Vol. 9, pp 71-144.

(67) Honig, B. H.; Hubbell, L.; Flewelling, R. F. *Annu. Rev. Biophys. Biophys. Chem.* 1986, 15, 163.

(60) van Buuren, A.; Berendsen, H. J. C. To be submitted for publication.

(61) van Buuren, A.; Marrink, S. J.; Berendsen, H. J. C., *J. Phys. Chem.*, in press.

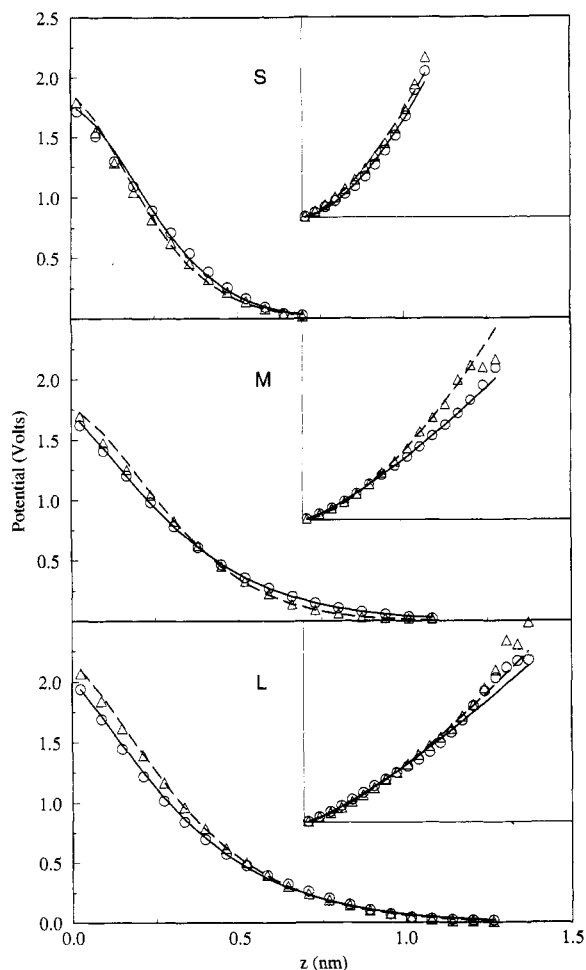


Figure 9. Fit from the interfacial plane of the electrostatic potentials to a stretched exponential for headgroups (triangles, dashed fit) and for water (circles, solid fit). The sign of the potentials of water is reversed for comparison. Inserted graphs show the same data but with a logarithmic y-axis. The parameters of the fits (for headgroups and water, respectively) are as follows: in simulation S, $\beta = 1.6$ and 1.7 , $l = 0.28$ and 0.31 nm; in simulation M, $\beta = 1.6$ and 1.3 , $l = 0.37$ and 0.37 nm; in simulation L, $\beta = 1.4$ and 1.3 , $l = 0.39$ and 0.39 nm.

observed in a simulation of a DPPC monolayer with excess water, using approximately the same simulation parameters.⁶⁸

Since all potential curves are very smooth as a result of the double integration, the fitting to exponential functions can be done quite accurately. However, for the total potential, being close to zero all the time, this is not the case. Nevertheless the actual decay of the total potential is determined by the decay of its constituent parts (lipid and water). We first tried to fit the curves to a single exponential, starting at the interfacial plane. We found a decay length of 0.4 nm, but the fit was not very good. Fitting the potential from the "border" plane gave a decay length of around 0.25 nm. So it seems that the decay length is not a constant but decreases toward the middle of the water layer. This can be clearly seen on a logarithmic scale (see Figure 9, inserted graphs). A single exponential decay would have resulted in a straight line of these plots, which is definitely not the case. Considering the still curved appearance of the potentials on a logarithmic scale, we therefore tried to fit the potential to a stretched exponential

$$\psi(z) = \psi_0 \exp[-(z/\lambda_{\text{str}})^\beta] \quad (8)$$

The result of this fit is also shown in Figure 9. As can be seen, the quality of the fit is very good, even on the

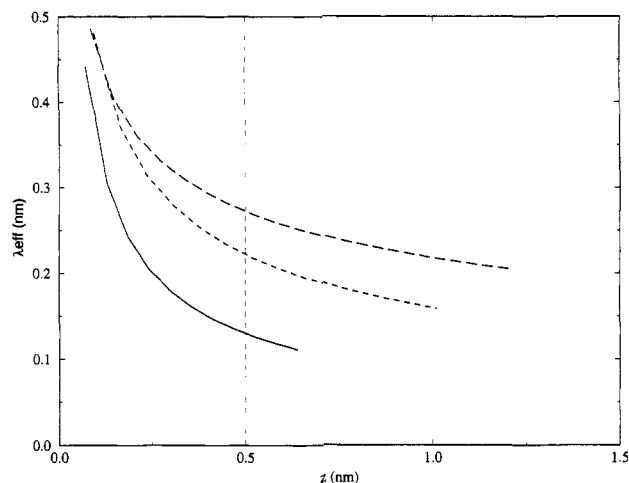


Figure 10. Local effective decay length of the electrostatic potentials with respect to the interfacial plane, in different systems: S (solid), M (dashed), L (long dashed). Border plane (dashed) is also shown. Curves were calculated from the fits to stretched exponentials (Figure 9).

logarithmic scale. The optimal values we found for the parameters λ_{str} ranged from 0.3 to 0.4 nm and for β from 1.3 to 1.7 (see legend of figure 9). The differences of these parameters for headgroup with respect to water potential are insignificant. The differences between the three simulations, however, seem to be significant and finds its origin probably in the differences in the interfacial charge distributions.

The physical meaning of the parameters λ_{str} and β is as yet unclear. A "local" decay length of the potentials can be extracted from the curves in Figure 9 by taking the derivative on a logarithmic scale, i.e. considering the stretched exponential locally as a single exponential with decay length $\lambda(z)$. The result of this calculation is shown in Figure 10. It clearly indicates a decreasing decay length, dropping from around 0.4 nm close to the interface to around 0.2 in the middle of the water layer.

V. Discussion

The first important feature to appear from our simulations is that the membrane/water interface is very rough indeed. The width of the interfacial region measures about 1.0 nm, which means that the thickness of the two interfacial regions comprises 40% of the total membrane! Just based on these numbers one could already conclude that the interface has to be modeled in *three* dimensions. This we also concluded from our MD study of the permeation of water through a lipid membrane,⁶⁹ modeled with the same system. Actually, the interface stretches out even further, as can be clearly seen from the graphical representation (Figure 2). Especially choline groups extend from the membrane quite far into the water layer. This picture resembles the schematic picture of the protrusion model.²⁷ However, neither our data on lipid mobility nor the distribution functions of headgroup atoms support the idea of an entropic confinement of the headgroups as the intermembrane distance gets smaller. However, our simulations are too short to include the effects of long-time diffusion. Hence the significance of entropic confinement cannot be assessed from our simulations.

From our analysis concerning the ordering of water, it is clear that the water structure is highly perturbed by the presence of the two membrane surfaces. Bulklike water is only found at a distance of 1.0 nm away from the

(68) Ahlström, P.; Berendsen, H. J. C. *J. Phys. Chem.*, in press.

interfacial plane. And even then, the hydrogen bonding pattern as well as diffusion rates still show some small, but significant, deviations.

The roughness and dynamical nature of the interface smear out the oscillatory behavior that is expected from the molecular nature of the system. The decay of all properties concerning the water ordering is therefore rather smooth. The largest decay occurs already within the interface itself. Moreover, it seems to be determined by the decay of the interface! Comparing for instance the decays of the orientational polarization (Figure 7) or the hydrogen bonding pattern (Figure 5a) with the decay of the choline density (Figure 3), it appears that they are all very similar, with a decay length around 0.25 nm.

The idea is affirmed by the behavior of the electrostatic potentials (Figure 8). They show that water molecules almost completely compensate for the potential arising from the lipid charges, over the full region where charges occur. It therefore seems that the water molecules are primarily ordered by the local charges of the lipid atoms. The decay length of this ordering will then naturally be the same as the decay length of the interfacial charges themselves. If any "intrinsic" decay length of water (whatever that means physically) would be of comparable or larger magnitude, we would have expected to see the water decay lagging behind the interfacial decay. Since we do not observe this, we conclude that the charge distribution due to local partial dipolar charges in the interfacial region directly determines the ordering of water molecules, overruling any "intrinsic" water decay.

This conclusion compares very well with the idea behind Ceve's model.⁶ Within this model, assuming that the interfacially induced decay of water is dominant, the hydration force will reflect the distribution of surface charges via the electrostatic potential. In order to get some insight into the hydration force in our system, it is therefore tempting to look at the decay characteristics of either the interfacial charges or their resulting potentials. The former possibility however poses the problem of which charges to choose. In first instance one could take the decay of just nitrogen atoms as being representative for the interfacial charge distributions. Its decay length around 0.23 nm nicely matches the experimental value of 0.21 nm for the decay length of the hydration force between DPPC membranes in the liquid-crystalline phase.¹⁸ But by considering only nitrogen atoms, any correlations between interfacial charges are neglected. This problem does not arise when the decay of the electrostatic potentials is considered, since all correlations are already incorporated. Besides, they are much smoother, so fitting can be done more accurately.

As we have seen, the electrostatic potentials can be fitted best to *stretched* exponentials instead of normal ones. These can be interpreted as having a continuously varying decay length instead of one single decay length. But where do they come from? Stretched exponentials appear in the description of the relaxation times in many diverse systems, such as dielectric relaxation in polymers, magnetization in spin glasses, and the decay of the luminescence in porous glasses.⁶⁹ The stretched exponential behavior is also appearing in the experiments and theory describing the double layer impedance,⁷⁰ and this is related

to the roughness of the surface and its fractal character. More generally, stretched exponentials are intimately connected to fractal properties of the underlying distribution.⁷¹ As we have seen from our simulations the phospholipid surfaces are very rough and therefore it is likely that a fractal description of the surfaces is appropriate. We shall limit ourselves to these remarks within the scope of the present article and address the fractal properties of membranes separately in the future.

An important consequence of the stretched exponential behavior is the appearance of a decreasing decay length. The question now is: how does this relate to the experimental¹⁸ observation of a single exponential with decay length of 0.21 nm and certainly not around 0.4 nm, the value we find in the interface? To us it seems that only the decay length of the tail of the potential functions is reflected in the measured hydration forces. Bringing the bilayers together, predominantly the unbound waters, i.e. the waters away from the interface, get squeezed out. The waters in the interfacial region are not likely to contribute. The experimental decay length is approximately observed over a distance range of 0.5–2.0 nm between the "border" planes. Within this range, the decay length of the electrostatic potentials is indeed around the experimental value. The difference between stretched exponential and single exponential behavior is probably too small to be derived from experiments. By use of data of Simon and McIntosh¹⁹ both types of fitting could be done with the same accuracy. Therefore, experiments probably only trace an effective decay length.

VI. Conclusions

From our simulations we conclude that the structure of water is perturbed by the presence of two phospholipid interfaces in the liquid-crystalline phase. This is evident from the results on orientation, hydrogen bonding, and diffusion. The ordering of water is smoothed out due to the broad and dynamic nature of these interfaces. Due to the broadness of the interface, the decay of water order is predominantly determined by the decay of the interfacial dipolar charge distribution. The electrostatic potentials arising from the charge distributions show a stretched exponential decay, which may be related to the fractal nature of the membrane/water interface. We expect that the hydration force exhibits the same type of decay, reflecting the detailed geometry of the interface. The hydration force thus will depend on both the solvent structure and the amount of protrusion of the lipids.

Acknowledgment. This work was partially supported by a grant from the Office of Naval Research and partially by the Foundation for Biophysics and the Foundation for National Computer Facilities under the auspices of the Netherlands Organization for Pure Research, NWO. The simulations were performed on the Cray-YMP at the North Carolina Supercomputing Center and on the Cray-YMP at the Computing Center of Amsterdam. M.B. is grateful to acknowledge the useful conversations with Prof. S. Simon and T. McIntosh.

(70) Liu, S. H.; Kaplan, T.; Gray, L. J. *Fractals in Physics*; Pietronero, L., Tosatti, E., Eds.; Elsevier: 1986; p 383.

(71) Takayasu, H. *Fractals in the Physical Sciences*; Holden, A. V., Ed.; Manchester University Press: Manchester, 1990; pp 123–130.

(69) Schlesinger, M. F.; Klafter, J. *Fractals in Physics*; Pietronero, L., Tosatti, E., Eds.; Elsevier: 1986; p 393.